

SELF-CONTACT SETS FOR 50 TIGHTLY KNOTTED AND LINKED TUBES

TED ASHTON, JASON CANTARELLA, MICHAEL PIATEK, AND ERIC RAWDON

ABSTRACT. We report on new numerical computations of the set of self-contacts in tightly knotted tubes of uniform circular cross-section. Such contact sets have been obtained before for the trefoil and figure eight knots by simulated annealing — we use constrained gradient-descent to provide new self-contact sets for those and 48 other knot and link types. The minimum length of all unit diameter tubes in a given knot or link type is called the ropelength of that class of curves. Our computations yield improved upper bounds for the ropelength of all knots and links with 9 or fewer crossings except the trefoil.

1. INTRODUCTION

The study of knots as abstract topological objects has inspired a great deal of fascinating mathematics. But knots are no less interesting as physical structures tied in flexible ropes and pulled tight. While it is intuitively clear that tight knots organize tension and contact forces to bind tightly and resist unravelling, the details of their structure remain mysterious. Even today, there is no explicit mathematical description of any tight knot.

We define the *thickness* of a space curve to be the supremal (largest) radius of any embedded tubular neighborhood of the curve, and the *ropelength* of a curve to be the quotient of its length and thickness. Ropelength provides a scale-invariant way to measure the total flexibility of a given length of rope. It has been established that there is a curve of minimum ropelength in each knot and link type L ([6, 5, 3]) and the ropelength of that curve is called the ropelength $\text{Rop}(L)$ of the knot or link type. These minimum ropelength curves are called *tight* or *ideal* knots. In this paper, we give some results from our numerical computations of the shapes of tight knots and links.

Over the past ten years, many authors have found approximate shapes for tight knots and links using numerical methods [9, 7, 4, 1]. We follow previous authors in defining a version of ropelength, Rop_p , for space polygons and optimizing this polygonal ropelength functional over the space of polygons in different knot and link types. But while most other others rely on simulated annealing, we introduce the use of constrained gradient descent for ropelength optimization.

This new method has allowed us to significantly expand the scope and accuracy of existing computations of tight knots. In particular, it seems that our method has succeeded at the challenging task of resolving the set of self-contacts in all knot and link types with nine and fewer crossings (212 types in all). In the process, we have produced a new table of upper bounds for the ropelengths of these knot and link types which improves upon previous results. These improvements range from 0.05% for the figure eight knot (compared to the bound of [4]) to more than 8.11% for the 9_{20} knot (compared to the bound of [13]). For links, these seem to be the first upper bounds reported for almost all of the link types we consider.

This dataset is likely to be useful in the study of tight knots, so we provide here an early view of our results. This research announcement will be followed by an expanded paper, “Tightening Knots with Constrained Gradient Descent”, which describes our methods and results in detail. The filesize limitations of the arXiv forced us to truncate the data section of this posting, and to use comparatively low-quality image files for the three-dimensional views of tight knots and links in Appendix B. A higher-quality view of these images is provided at http://www.cs.washington.edu/homes/piatek/contact_table/.

Date: June 12, 2004; Revised: July 13, 2018.

Key words and phrases. ropelength, tight knots, ideal knots, self-contact sets, knot-tightening.

2. BACKGROUND MATERIAL

We start by defining ropelength more precisely. Suppose γ is a C^1 space curve, parameterized by arclength. The maximum diameter of an embedded tube around γ is controlled by two phenomena: “self-contacts” of the tube formed when sections of the curve far away in arclength approach each other in space, and “kinks” formed by points of high curvature on γ . These effects are shown below in Figure 1.

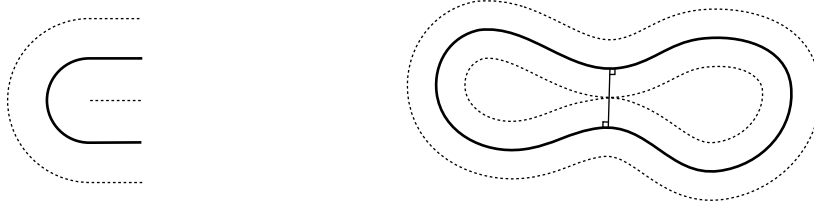


FIGURE 1. The thickness of a smooth curve γ is controlled by curvature (as in the left picture), and self-contacts of the tube around γ (as in the right picture).

To make this understanding precise, we need a few definitions. We can define the self-distance map of γ by

$$d(s, t) = \|\gamma(s) - \gamma(t)\|.$$

We then have

Definition 1. The set $\text{dcsd}(\gamma)$ of *doubly-critical self-distances* of γ is the set of critical points for $d(s, t)$ with $s \neq t$. Taking the partial derivatives of d , we see that $(s, t) \in \text{dcsd}(\gamma)$ if and only if

$$\langle \gamma(s) - \gamma(t), \gamma'(s) \rangle = 0 \text{ and } \langle \gamma(s) - \gamma(t), \gamma'(t) \rangle = 0.$$

Denoting the curvature of γ at s by $\kappa(s)$, Litherland et al. proved

Theorem 2.1. [8] *The thickness of γ is the minimum of*

$$\min_s \frac{1}{\kappa(s)} \text{ and } \min_{(s,t) \in \text{dcsd}(\gamma)} \frac{d(s, t)}{2}.$$

We can now define the primary object of interest in our computations:

Definition 2. The *self-contact set* or *strut set* of a space curve γ is the set of $(s, t) \in \text{dcsd}(\gamma)$ with $\|\gamma(s) - \gamma(t)\| = 2 \text{Thi}(\gamma)$.

The term “strut”, borrowed from tensegrity theory, comes from the fact that minimum-length chords in $\text{dcsd}(\gamma)$ “hold the curve apart from itself” as the knot tightens.

In our polygonal knot-tightening problem, we will replace the curve γ with a space polygon \mathcal{V} with vertices v_1, \dots, v_V and edges e_1, \dots, e_V . To define the polygonal thickness $\text{Thi}_p(\mathcal{V})$ of \mathcal{V} , we will need an idea of curvature.

Definition 3. The minimum radius of curvature (or MinRad) of \mathcal{V} at v_i is given by the radius of the unique circle tangent to both of the edges which meet at v_i and passing through the midpoint of the shorter one.

If θ_i is the turning angle of \mathcal{V} at v_i , then $\text{MinRad}(v_i)$ is given by

$$\text{MinRad}(v_i) = \frac{\min\{|e_{i-1}|, |e_i|\}}{2 \tan(\theta_i/2)}.$$

We will also need a definition of doubly-critical self-distances:

Definition 4. Let $\text{dcsd}(\mathcal{V})$ be the set of (p, q) on \mathcal{V} with $p \neq q$ which are local minima of the self-distance function.

We now define a thickness measure for polygons:

Definition 5. The thickness $\text{Thi}_p(\mathcal{V})$ of a space polygon \mathcal{V} without self-intersections is given by the minimum of

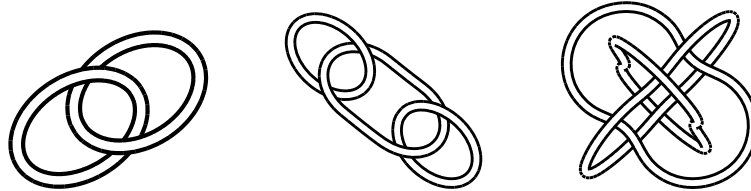
$$\min_i \text{MinRad}(v_i) \quad \text{and} \quad \min_{(p,q) \in \text{dcsd}(\mathcal{V})} \frac{d(p,q)}{2}.$$

The polygonal ropelength Rop_p of \mathcal{V} is then the quotient of the length of \mathcal{V} and $\text{Thi}_p(\mathcal{V})$. As expected, when polygons \mathcal{V}_n with increasing numbers of edges are inscribed in a space curve γ , it is known that $\text{Rop}_p(\mathcal{V}_n) \rightarrow \text{Rop}(\gamma)$ under some mild geometric hypotheses [10, 12, 13]. We define self-contact sets for polygons like we do for smooth curves.

3. QUANTITIES COMPUTED AND HOW THE COMPUTATION WAS VALIDATED

Our algorithm minimizes the length of \mathcal{V} subject to a family of constraints derived from the distance and MinRad functions in Definition 5. We report the polygonal ropelengths of the minimized configurations in summary form in Appendix A. We also report preliminary computations of the ropelengths of piecewise-smooth curves obtained from our polygons by replacing the corners of the polygon with small circular arcs. These provide tentative upper bounds on the ropelengths of the knot and link types listed. We also provide self-contact sets for 50 of these knots and links.

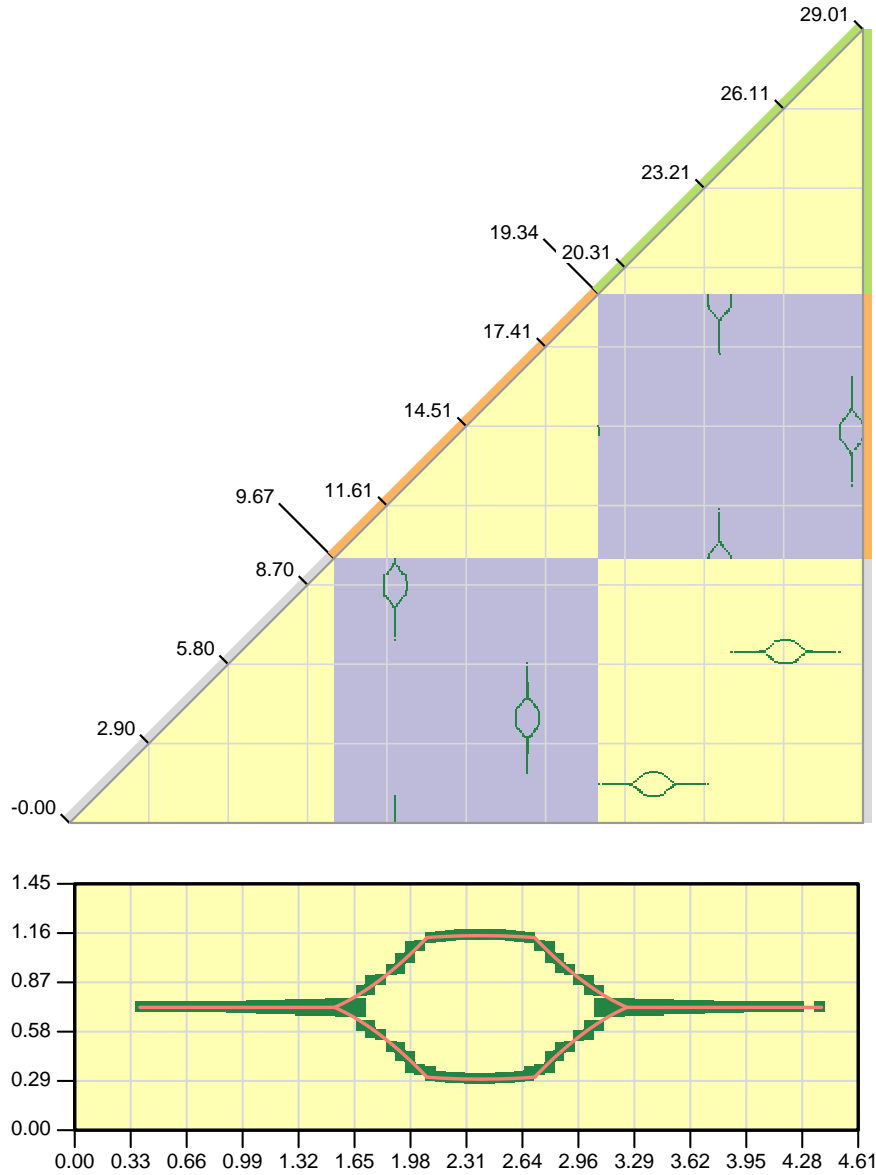
Though our ropelength bounds for knots improve on those of previous authors, this is an uncertain measure of their quality. After all, there is no way to check the accuracy of an upper bound for the ropelength of any knot, since no exact value for the minimum ropelength of any knot type is known. On the other hand, the minimum ropelength is known or explicitly conjectured for some link types [3, 2]. A comparison of our results to some of these known examples appears below.



Link name	Hopf link (2_1)	3-link chain ($2_1 \# 2_1$)	Borromean rings (6_3^2)
Edges	216	384	630
Polygon length	25.1439	41.7131	58.0300
Upper bound	25.1388	41.7086588	58.0145
Smooth length	8π	$12\pi + 4$	58.006
Relative error	0.02%	0.02%	0.01%

The results above lead us to suspect that most of our smooth ropelength bounds are within 1 to 2 hundredths of a percent of the corresponding minimum ropelength values, but we must be cautious. The ropelength “landscape” for knots is quite complicated, and we have already discovered a number of local ropelength minima for 8 and 9-crossing knots which are very different from the (apparent) global ropelength minima for these knot types. If our gradient descent algorithm has been trapped by one of these local minima, the figures we report might be an accurate computation of the ropelength of the local minimizer, but far off from the true minimum ropelength value for the knot type.

We checked our computation of the self-contact sets by comparing our computed self contact set for the Borromean rings to the contact set for the ropelength-critical configuration provided by [2]. The results appear in the Figure below.



The polygonal configuration of the Borromean rings discovered by our software has total length about 29.01. The top plot shows the lower triangle of the square $[0, 29.01] \times [0, 29.01]$ representing pairs of arclength values (s, t) on these polygonal rings. To describe the position of a point on this 3-component link with a single arclength value, we use the convention that arclength values in $[0, 9.67)$ refer to points on the first component, values in $[9.67, 19.34)$ refer to points on the second component, and values in $[19.34, 29.01)$ refer to points on the third component of the link. These breaks are reinforced by the colored bands running up the diagonal of the plot, which correspond to the colors of the different components of our tight links in the 3d renderings of Appendix B.

The s and t position of points on the plot is indicated by the labels running up the diagonal, where the three special values representing breaks between components are lifted away from the other labels. The breaks between components are also shown on the plot by the alternating checkerboard pattern of the background colors.

We then locate every pair $(s, t) \in \text{dcsd}(\mathcal{V})$ with $\|\mathcal{V}(s) - \mathcal{V}(t)\| \leq \text{Thi}_p(\mathcal{V}) + 10^{-5}$. In the context of our gradient descent algorithm, these points represent active distance constraints. Our code computes Lagrange multipliers for all these active constraints, which represent self-contact forces borne by these tube contacts in the tight knot. We center

a dark green box at every such (s, t) value with a nonzero Lagrange multiplier. The size of the box represents the average¹ edglength of the polygon \mathcal{V} . We chose this size to represent the expected error in computed self-contact positions introduced by approximating a C^1 ropelength-minimizer by the polygon \mathcal{V} .

As we see from the plot, no tube around a component of the link is in contact with itself (so the three cream-colored triangles near the diagonal are empty). But each of the components makes contact with the other two, as shown by the boxes plotted in the purple and cream-colored rectangles forming the remainder of the plot. We can see that the contacts break up naturally into “lantern-shaped” structures.

This link has been studied by Cantarella, Fu, Kusner, Sullivan, and Wrinkle, who provide a ropelength-critical configuration in [2]. In the bottom plot, we compare one “lantern” formed by 608 of these boxes to the self-contact set predicted by these authors, which is represented by a red line. In this plot, the arclength distances labelled on the s and t axes do not correspond to a region of the plot above, but merely indicate the scale of the plot. We can see that the agreement between theory and computation is generally within one edglength.

Appendix B contains similar plots of our computed self-contact sets for 50 knots and links from our collection of minimized examples. To the left of each self-contact plot, we provide a 3d rendering of the corresponding tight shape. For links, the diagonal and right-hand side of the triangular self-contact plot are colored gray, orange and green in correspondance with the colors of the components in the rendering. The start of each component in the rendering is denoted by the tube coming to a point. The black bands on the tubes correspond to the arclength tick marks on the plot at right. The table also contains the polygonal ropelength of the knot (top number, slightly higher) and the corresponding smooth ropelength upper bound (bottom number, slightly lower), as well as the number of edges in the configuration plotted.

4. CONCLUSIONS

The major contribution of Appendix A is the provision of ropelength figures for links. This allows us to check the accuracy of numerical ropelength minimizations against theoretical results for the first time. We are happy to report that our method passes this test for the cases we examined.

The pictures in Appendix B are considerably more evocative. It is evident from first inspection that the contact sets of tight knots and links seem to contain a fairly small number of commonly repeated patterns. Some of these, such as the “steps” pattern first seen in the trefoil knot, change shape from knot to knot. But others (such as the “winged” pattern in the figure eight knot or the “lantern” shape seem in the Borromean rings) seem to remain remarkably consistent throughout our computations. The reader may notice many other examples as well. Isolating and understanding some of these structures could provide us with a “construction kit” for tight knots, much like the analysis of the simple chain in [3] led to the construction of an infinite family of tight links.

5. ACKNOWLEDGEMENTS

We would like to acknowledge many helpful conversations with our colleagues during the years we spent working on this project. In particular, Mark Peletier and Bob Planque, John Sullivan, Erik Demaine and Bob Connelly, Herbert Edelsbrunner, and Joe Fu all provided helpful insights and advice at various points in the process. We were supported by NSF grants DMS-02-04826 (to Cantarella and Fu), DMS-00-89927 (the University of Georgia VIGRE grant), and DMS-03-11010 (to Rawdon).

¹Our final polygons are almost-equilateral, so this is a good approximation of the lengths of the edges incident to the pair (s, t) .

REFERENCES

- [1] Justyna Baranska, Piotr Pieranski, Sylwester Przybyl, and Eric J. Rawdon. Length of the tightest trefoil knot. *Physical Review E (Statistical, Nonlinear, and Soft Matter Physics)*, 70(5):051810, 2004.
- [2] Jason Cantarella, Joseph H.G. Fu, Robert B. Kusner, John M. Sullivan, and Nancy C. Wrinkle. Criticality for the Gehring link problem. arXiv:math.DG/0402212.
- [3] Jason Cantarella, Robert B. Kusner, and John M. Sullivan. On the minimum ropelength of knots and links. *Invent. Math.*, 150(2):257–286, 2002.
- [4] M. Carlen, B. Laurie, J.H. Maddocks, and J. Smutny. *Biarcs, Global Radius of Curvature, and the Computation of Ideal Knot Shapes*. World Scientific, 2005.
- [5] O. Gonzalez and R. de la Llave. Existence of ideal knots. *J. Knot Theory Ramifications*, 12(1):123–133, 2003.
- [6] O. Gonzalez, J. H. Maddocks, F. Schuricht, and H. von der Mosel. Global curvature and self-contact of nonlinearly elastic curves and rods. *Calc. Var. Partial Differential Equations*, 14(1):29–68, 2002.
- [7] Ben Laurie. Annealing ideal knots and links: methods and pitfalls. In *Ideal knots*, volume 19 of *Ser. Knots Everything*, pages 42–51. World Sci. Publishing, River Edge, NJ, 1998.
- [8] R. A. Litherland, J. Simon, O. Durumeric, and E. Rawdon. Thickness of knots. *Topology Appl.*, 91(3):233–244, 1999.
- [9] Piotr Pierański. In search of ideal knots. In *Ideal knots*, volume 19 of *Ser. Knots Everything*, pages 20–41. World Sci. Publishing, River Edge, NJ, 1998.
- [10] Eric Rawdon. *The Thickness of Polygonal Knots*. PhD thesis, The University of Iowa, 1997.
- [11] Eric Rawdon and Michael Piatek. Data from the TOROS system for 9-crossing knots. 2005.
- [12] Eric J. Rawdon. Approximating the thickness of a knot. In *Ideal knots*, volume 19 of *Ser. Knots Everything*, pages 143–150. World Sci. Publishing, River Edge, NJ, 1998.
- [13] Eric J. Rawdon. Can computers discover ideal knots? *Experiment. Math.*, 12(3):287–302, 2003.

Ted Ashton and Jason Cantarella
Department of Mathematics, University of Georgia, Athens GA

Michael Piatek
Department of Computer Science, University of Washington, Seattle WA

Eric Rawdon
Department of Mathematics, Duquesne University, Pittsburgh, PA

APPENDIX A. TABLE OF POLYGONAL ROPELENGTHS AND ROPELENGTH UPPER BOUNDS

The table shows new polygonal ropelengths and ropelength upper bounds for 212 knots and links with 9 or fewer crossings. From left to right, there are four columns: the name of the knot or link, the polygonal ropelength Rop_p , the corresponding ropelength upper bound Rop , and the previous best ropelength upper bound we could find in the literature together with the percentage improvement in ropelength. For these last figures, we used the papers [1, 4, 11].

Link	Rop_p	Rop	Previous	Link	Rop_p	Rop	Previous
2_1^2	25.1439	25.1388		8_3	71.1880	71.1655	71.56 (0.55%)
3_1	32.7490	32.7448	32.7433864 (-%)	8_4	72.0301	72.0049	72.41 (0.55%)
4_1	42.0997	42.0928	42.1158845 (0.05%)	8_5	72.2100	72.1878	72.70 (0.7%)
4_1^2	40.0247	40.0169		8_6	72.5005	72.4791	72.93 (0.61%)
5_1	47.2156	47.2016	47.51 (0.64%)	8_7	72.2447	72.2204	72.63 (0.56%)
5_2	49.4840	49.4704	49.73 (0.52%)	8_8	73.3533	73.3334	73.88 (0.73%)
5_1^2	49.7874	49.7723		8_9	72.4717	72.4461	72.96 (0.7%)
6_1	56.7316	56.7150	57.11 (0.69%)	8_{10}	73.4279	73.4095	73.86 (0.6%)
6_2	57.0451	57.0271	57.44 (0.71%)	8_{11}	73.5029	73.4802	76.70 (4.19%)
6_3	57.8602	57.8435	58.48 (1.08%)	8_{12}	74.0291	74.0098	74.61 (0.8%)
6_1^2	54.4068	54.3893		8_{13}	72.8291	72.8045	73.29 (0.66%)
6_2^2	56.7132	56.7028		8_{14}	73.9226	73.8991	74.93 (1.37%)
6_3^2	58.1161	58.1044		8_{15}	74.3344	74.3134	74.82 (0.67%)
6_1^3	57.8334	57.8170		8_{16}	74.9213	74.8962	75.47 (0.76%)
6_2^3	58.0300	58.0145		8_{17}	74.5276	74.5071	75.08 (0.76%)
6_3^3	50.5865	50.5745		8_{18}	74.9420	74.9252	75.44 (0.68%)
7_1	61.4319	61.4109	61.89 (0.77%)	8_{19}	61.0734	61.0430	61.35 (0.5%)
7_2	63.9165	63.8956	65.36 (2.24%)	8_{20}	63.1530	63.1146	64.11 (1.55%)
7_3	63.9539	63.9327	64.35 (0.64%)	8_{21}	65.5504	65.5298	65.91 (0.57%)
7_4	64.2960	64.2724	65.63 (2.06%)	8_1^2	68.5198	68.4884	
7_5	65.2802	65.2609	65.70 (0.66%)	8_2^2	71.1823	71.1587	
7_6	65.7183	65.7012	66.17 (0.7%)	8_3^2	72.7498	72.7291	
7_7	65.6316	65.6108	66.09 (0.72%)	8_4^2	72.6102	72.5908	
7_1^2	64.2585	64.2353		8_5^2	74.0039	73.9826	
7_2^2	65.0467	65.0274		8_6^2	73.2932	73.2502	
7_3^2	65.3743	65.3561		8_7^2	74.4165	74.3885	
7_4^2	65.0971	65.0759		8_8^2	73.7849	73.7702	
7_5^2	66.2400	66.2186		8_9^2	74.0620	74.0386	
7_6^2	66.3494	66.3372		8_{10}^2	73.6890	73.6684	
7_7^2	55.5451	55.5311		8_{11}^2	73.0115	72.9899	
7_8^2	57.8043	57.7948		8_{12}^2	74.0194	73.9140	
7_1^3	65.8275	65.8090		8_{13}^2	74.1685	74.1501	
8_1	71.0484	71.0241	71.44 (0.58%)	8_{14}^2	73.7000	73.6775	
8_2	71.4327	71.4107	71.91 (0.69%)	8_{15}^2	64.3305	64.3086	
				8_{16}^2	66.8434	66.8315	
				8_1^3	72.2883	72.2649	
				8_2^3	72.9544	72.9360	
				8_3^3	74.9366	74.9139	
				8_4^3	77.8544	77.8314	
				8_5^3	73.4286	73.4061	
				8_6^3	74.7680	74.7468	
				8_7^3	60.6065	60.5888	

Link	Rop _p	Rop	Previous
8 ₈ ³	65.0637	65.0444	
8 ₉ ³	70.1904	70.1810	
8 ₁₀ ³	68.9823	68.9694	
8 ₁ ⁴	75.2901	75.2677	
8 ₂ ⁴	67.4772	67.4571	
8 ₃ ⁴	66.4140	66.4046	
9 ₁	75.7507	75.7252	76.43 (0.92%)
9 ₂	79.3059	79.2794	79.92 (0.8%)
9 ₃	78.5867	78.5591	79.05 (0.62%)
9 ₄	78.4117	78.3861	78.84 (0.57%)
9 ₅	79.7877	79.7586	80.32 (0.69%)
9 ₆	80.1326	80.0822	80.65 (0.7%)
9 ₇	80.6597	80.6357	82.65 (2.43%)
9 ₈	80.5651	80.5384	81.14 (0.74%)
9 ₉	79.9574	79.9323	80.85 (1.13%)
9 ₁₀	79.8161	79.7946	80.33 (0.66%)
9 ₁₁	80.3650	80.3418	81.98 (1.99%)
9 ₁₂	80.1275	80.1047	80.71 (0.74%)
9 ₁₃	80.6525	80.6246	81.33 (0.86%)
9 ₁₄	80.1512	80.1259	80.73 (0.74%)
9 ₁₅	82.1665	82.1396	82.70 (0.67%)
9 ₁₆	80.1446	80.1211	80.67 (0.68%)
9 ₁₇	80.5792	80.5537	81.90 (1.64%)
9 ₁₈	81.6230	81.5960	82.68 (1.31%)
9 ₁₉	82.1828	82.1593	82.72 (0.67%)
9 ₂₀	80.2543	80.2288	87.31 (8.11%)
9 ₂₁	81.1336	81.1098	81.64 (0.64%)
9 ₂₂	81.0714	81.0464	81.60 (0.67%)
9 ₂₃	81.3164	81.2898	81.84 (0.67%)
9 ₂₄	80.9933	80.9701	81.54 (0.69%)
9 ₂₅	81.1873	81.1612	81.85 (0.84%)
9 ₂₆	80.9352	80.9137	81.94 (1.25%)
9 ₂₇	81.9473	81.9092	83.21 (1.56%)
9 ₂₈	81.5694	81.5467	82.25 (0.85%)
9 ₂₉	81.8708	81.8470	83.45 (1.92%)
9 ₃₀	81.8567	81.8344	82.46 (0.75%)
9 ₃₁	81.7436	81.6915	82.22 (0.64%)
9 ₃₂	81.5775	81.5555	82.34 (0.95%)
9 ₃₃	82.8451	82.7989	83.37 (0.68%)
9 ₃₄	82.3213	82.2744	82.99 (0.86%)
9 ₃₅	79.2495	79.2216	80.85 (2.01%)
9 ₃₆	81.0579	81.0297	81.57 (0.66%)
9 ₃₇	81.5845	81.5562	82.10 (0.66%)
9 ₃₈	81.8119	81.7909	82.43 (0.77%)
9 ₃₉	81.9490	81.9266	85.55 (4.23%)
9 ₄₀	81.7008	81.6806	82.67 (1.19%)
9 ₄₁	81.4929	81.4399	82.11 (0.81%)
9 ₄₂	69.6133	69.5939	70.02 (0.6%)
9 ₄₃	71.7062	71.6863	72.20 (0.71%)

Link	Rop _p	Rop	Previous
9 ₄₄	71.6516	71.6305	72.23 (0.82%)
9 ₄₅	74.9154	74.8959	75.51 (0.81%)
9 ₄₆	68.6579	68.6369	69.35 (1.02%)
9 ₄₇	75.1289	75.0875	75.61 (0.69%)
9 ₄₈	74.2918	74.2477	74.94 (0.92%)
9 ₄₉	74.0530	74.0127	74.50 (0.65%)
9 ₁ ²	78.7014	78.6731	
9 ₂ ²	79.5525	79.5259	
9 ₃ ²	79.9725	79.9476	
9 ₄ ²	78.7248	78.6967	
9 ₅ ²	79.6807	79.6549	
9 ₆ ²	81.1029	81.0791	
9 ₇ ²	81.1705	81.1460	
9 ₈ ²	81.0999	81.0723	
9 ₉ ²	80.3391	80.3181	
9 ₁₀ ²	80.3964	80.3693	
9 ₁₁ ²	82.0513	82.0271	
9 ₁₂ ²	81.9983	81.9738	
9 ₁₃ ²	79.3586	79.3319	
9 ₁₄ ²	80.7420	80.7171	
9 ₁₅ ²	80.5805	80.5550	
9 ₁₆ ²	81.4190	81.3966	
9 ₁₇ ²	81.2589	81.2307	
9 ₁₈ ²	82.2739	82.2429	
9 ₁₉ ²	79.4899	79.4628	
9 ₂₀ ²	80.4176	80.3956	
9 ₂₁ ²	81.2545	81.2356	
9 ₂₂ ²	81.1318	81.1058	
9 ₂₃ ²	80.4552	80.4290	
9 ₂₄ ²	82.5780	82.5207	
9 ₂₅ ²	81.8205	81.7924	
9 ₂₆ ²	82.1200	82.1015	
9 ₂₇ ²	81.3442	81.2046	
9 ₂₈ ²	81.3869	81.3740	
9 ₂₉ ²	82.1780	82.1567	
9 ₃₀ ²	82.2789	82.2517	
9 ₃₁ ²	80.6125	80.5936	
9 ₃₂ ²	81.4352	81.4122	
9 ₃₃ ²	82.2167	82.1951	
9 ₃₄ ²	81.8743	81.8552	
9 ₃₅ ²	81.3504	81.3284	
9 ₃₆ ²	80.7280	80.7103	
9 ₃₇ ²	81.9353	81.9101	
9 ₃₈ ²	82.7480	82.7206	
9 ₃₉ ²	81.9251	81.8973	
9 ₄₀ ²	82.0090	81.9822	
9 ₄₁ ²	83.6167	83.5979	
9 ₄₂ ²	83.6493	83.6292	
9 ₄₃ ²	66.3264	66.3049	
9 ₄₄ ²	72.2518	72.2255	

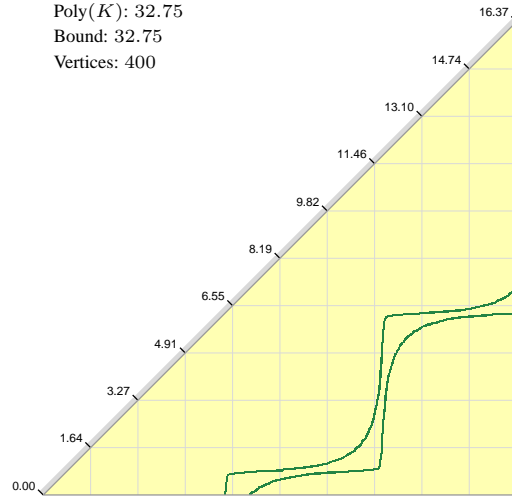
Link	Rop _p	Rop	Previous
9_{45}^2	71.3593	71.3490	
9_{46}^2	73.9646	73.9377	
9_{47}^2	69.9602	69.9432	
9_{48}^2	73.6781	73.6545	
9_{49}^2	66.0806	66.0658	
9_{50}^2	69.3690	69.3483	
9_{51}^2	70.5942	70.5699	
9_{52}^2	72.9916	72.9685	
9_{53}^2	68.0369	68.0305	
9_{54}^2	71.0385	71.0185	
9_{55}^2	73.8423	73.8217	
9_{56}^2	75.2439	75.2245	
9_{57}^2	73.8408	73.8194	
9_{58}^2	74.1911	74.1697	
9_{59}^2	73.0481	73.0305	
9_{60}^2	73.5734	73.5553	
9_{61}^2	69.3978	69.3840	
9_3^3	81.2897	81.2323	
9_2^3	82.4507	82.4004	
9_3^3	82.3127	82.2861	
9_4^3	82.5449	82.5208	
9_5^3	80.7974	80.7714	
9_6^3	81.0235	81.0054	
9_7^3	82.1986	82.1535	
9_8^3	81.1631	81.1408	
9_9^3	81.6200	81.5735	
9_{10}^3	82.3446	82.3259	
9_{11}^3	82.0323	82.0137	
9_{12}^3	82.6345	82.5740	
9_{13}^3	72.2098	72.2008	
9_{14}^3	74.5697	74.5492	
9_{15}^3	74.3877	74.3655	
9_{16}^3	75.0664	75.0430	
9_{17}^3	74.2972	74.2779	
9_{18}^3	72.5059	72.4741	
9_{19}^3	72.7143	72.6859	
9_{20}^3	76.3557	76.1829	
9_{21}^3	74.9369	74.9212	
9_1^4	85.5620	85.5115	

APPENDIX B. TABLE OF SELF-CONTACT SETS

3_1



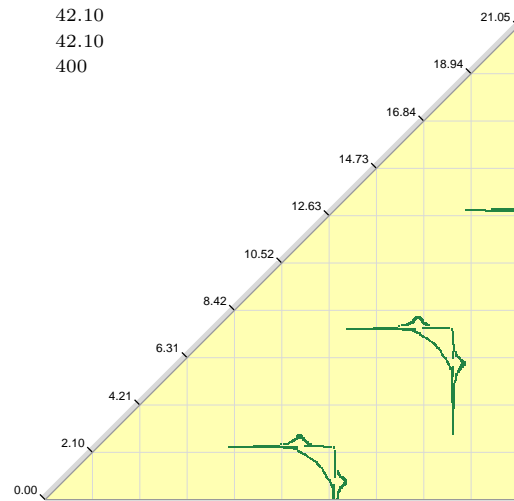
Poly(K): 32.75
Bound: 32.75
Vertices: 400



4_1



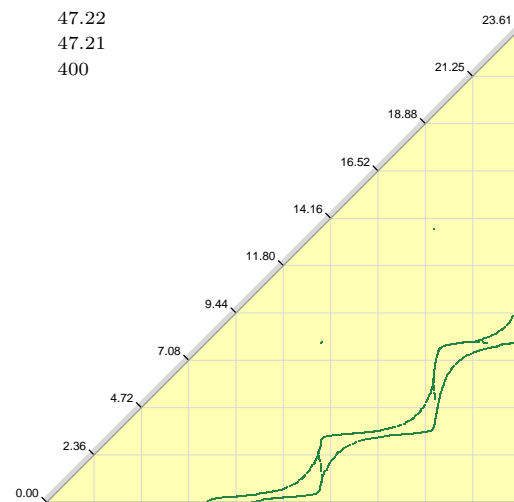
42.10
42.10
400



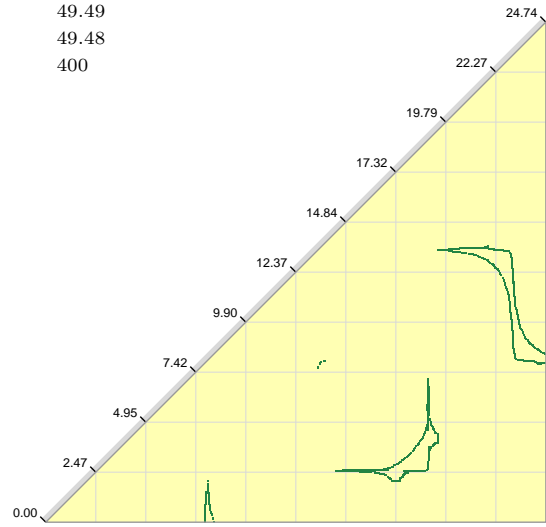
5_1



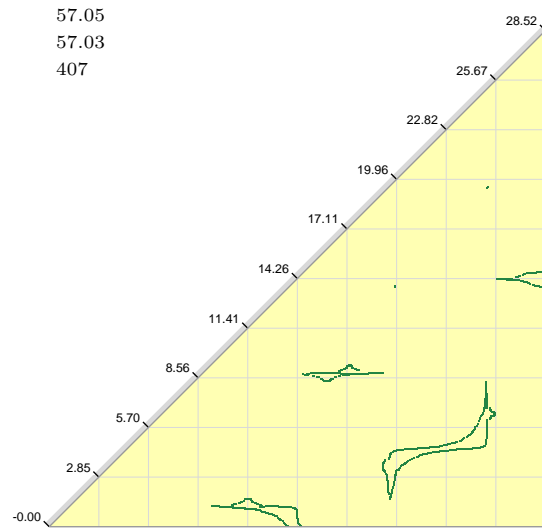
47.22
47.21
400



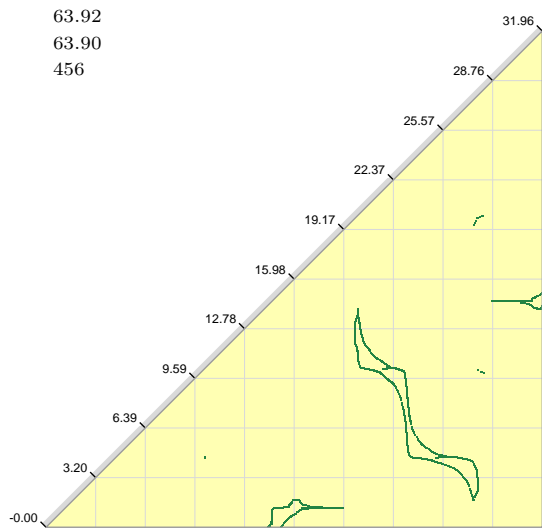
5₂



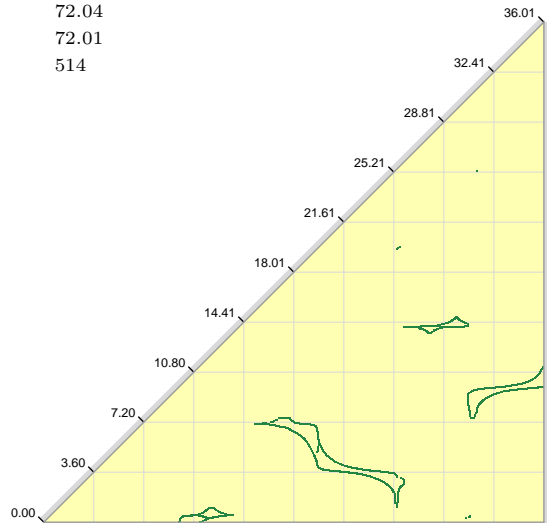
6₂



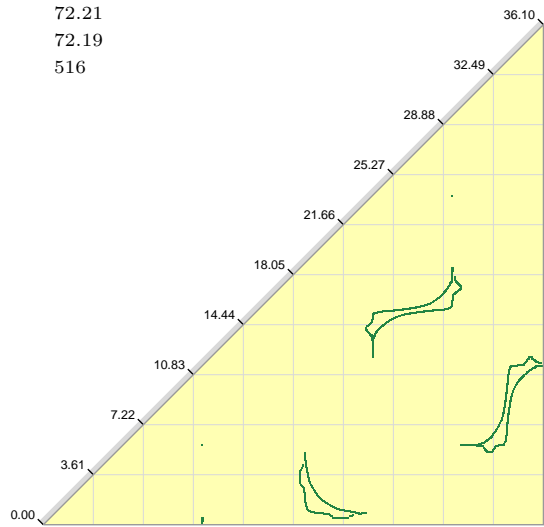
7₂



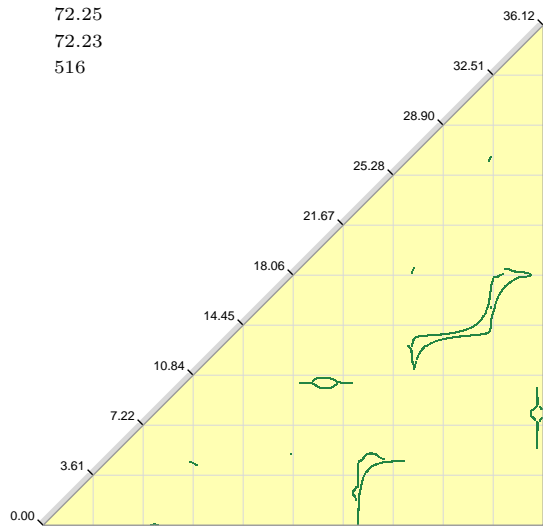
8₄



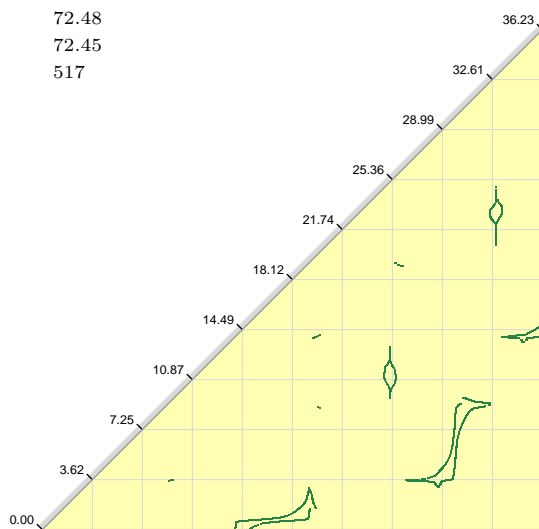
8₅



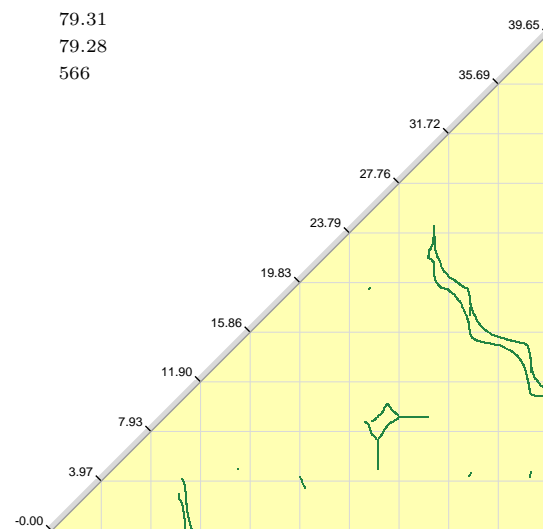
8₇



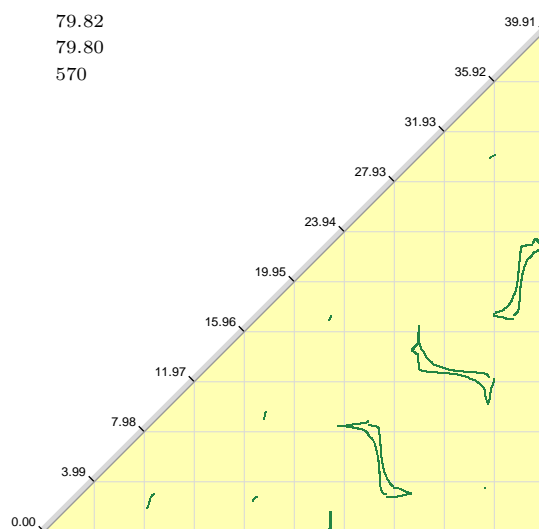
8₉



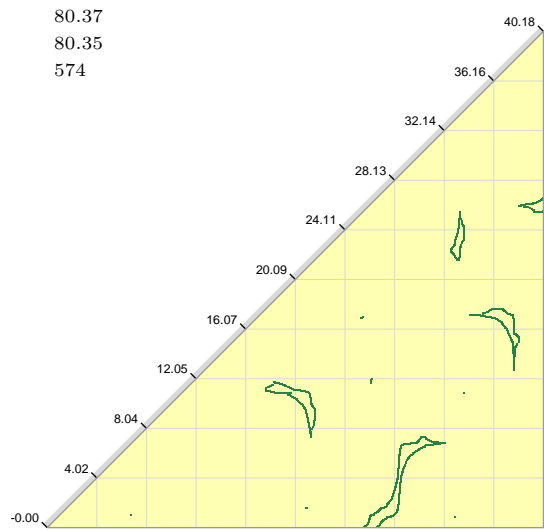
9₂



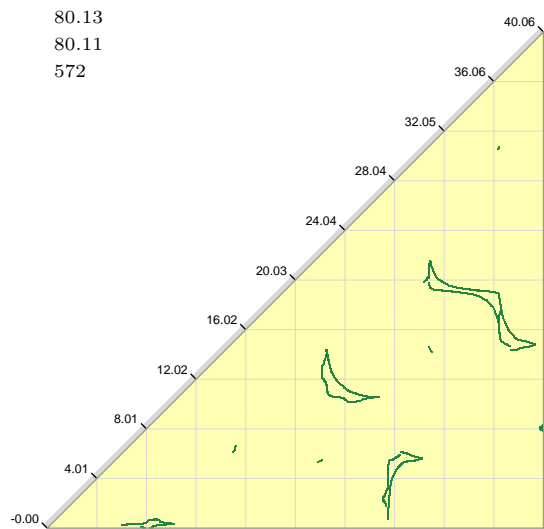
9₁₀



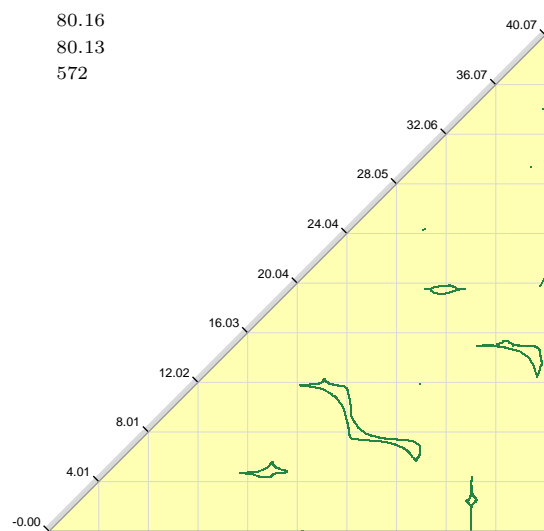
9₁₁



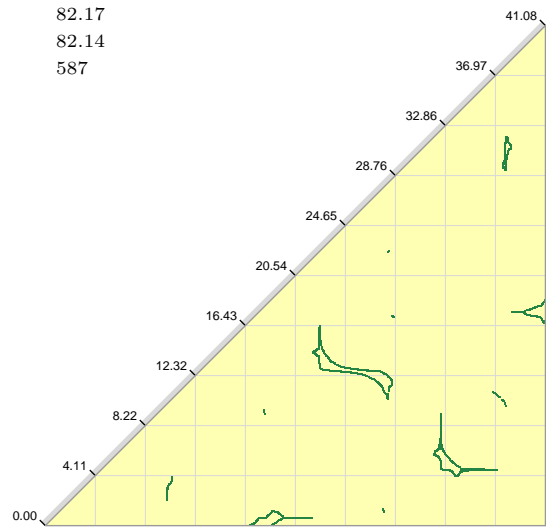
9₁₂



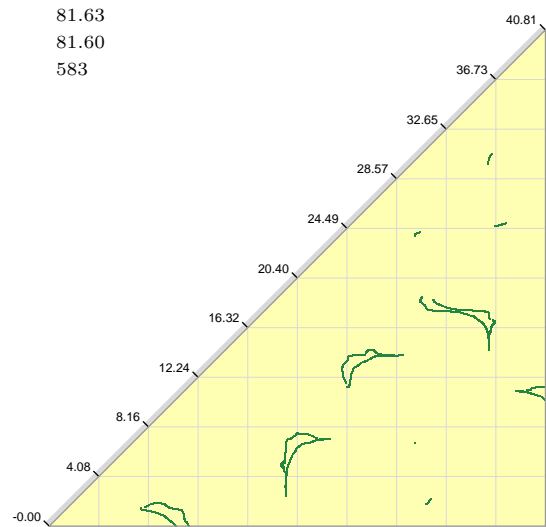
9₁₄



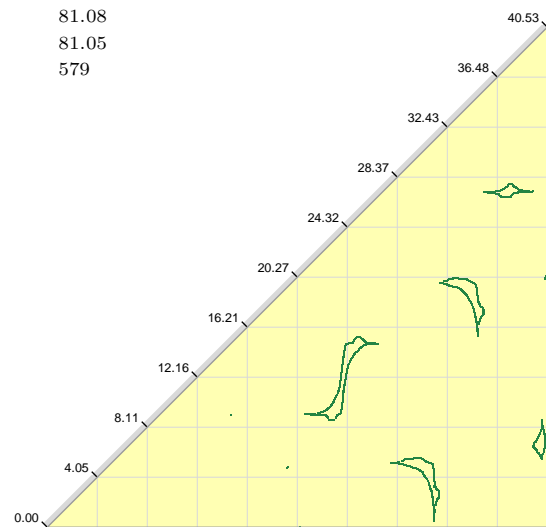
9₁₅



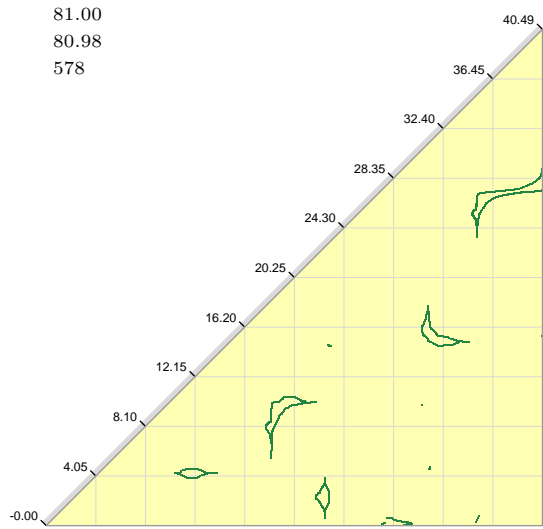
9₁₈



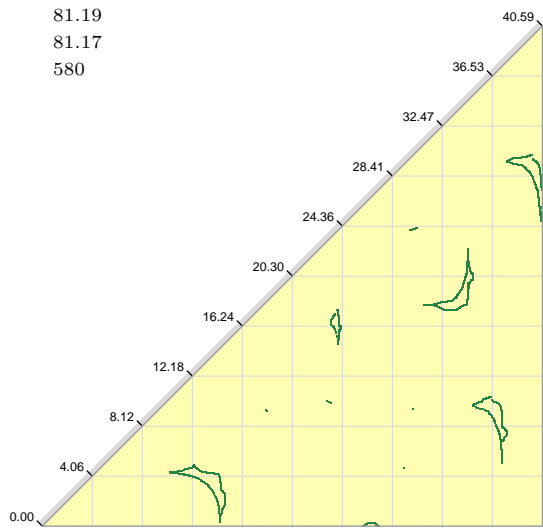
9₂₂



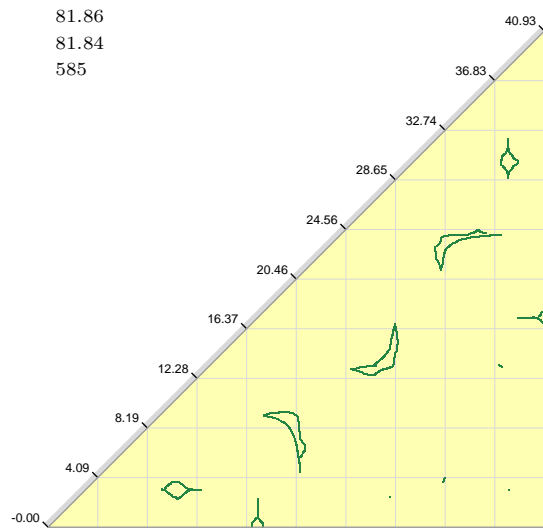
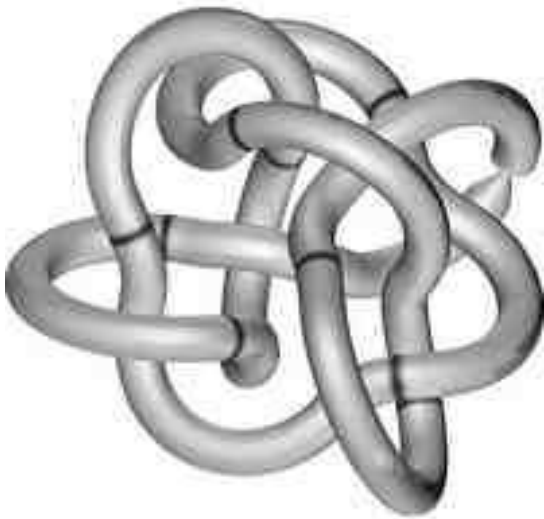
9₂₄



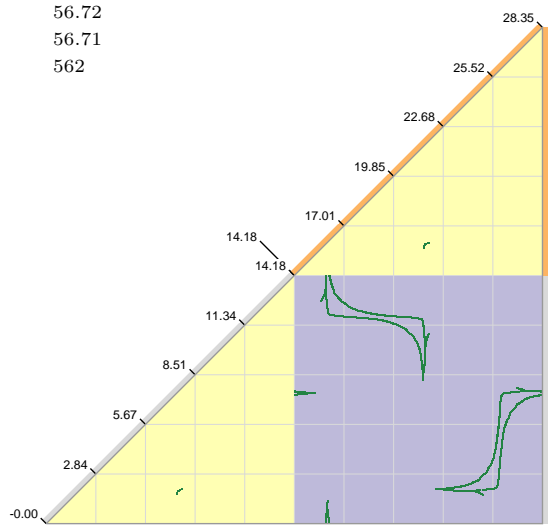
9₂₅



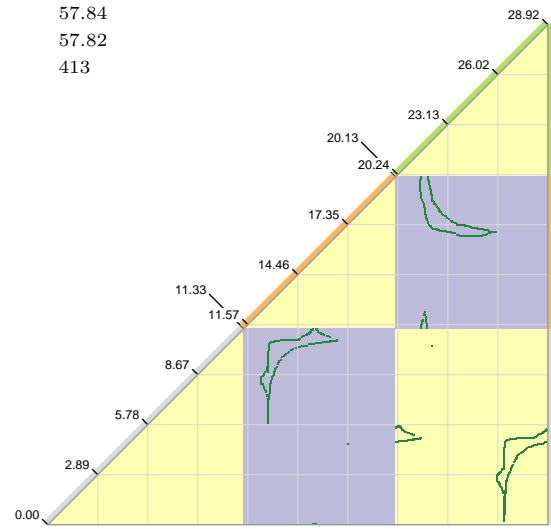
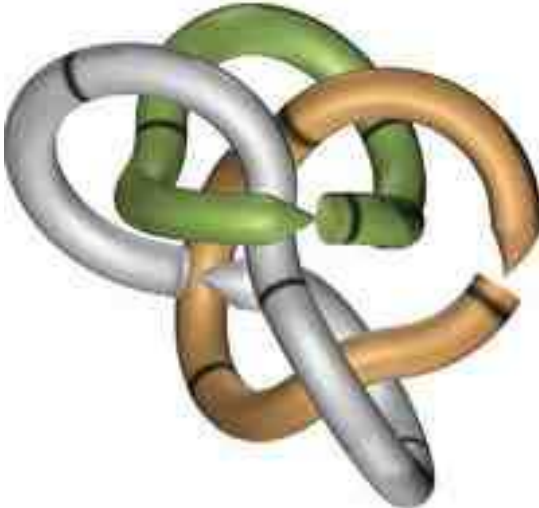
9₃₀



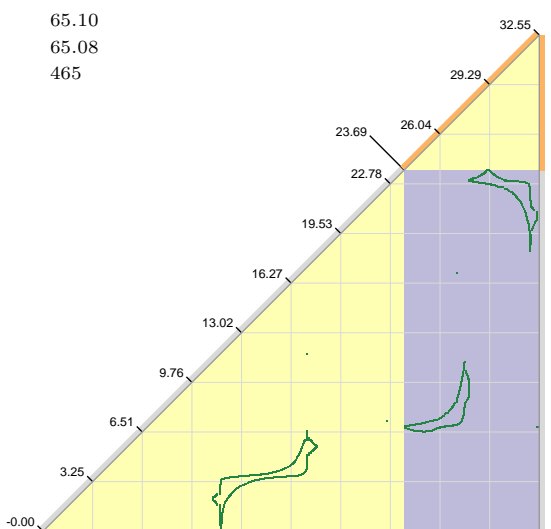
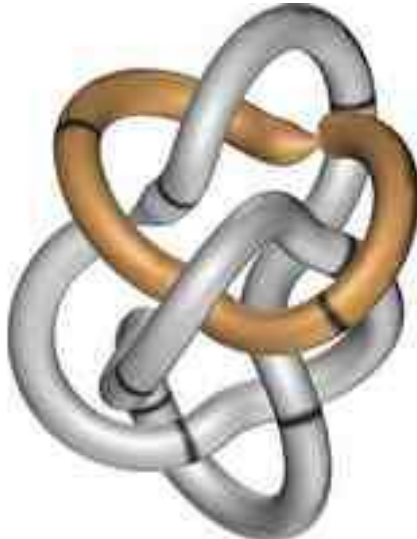
6_2^2



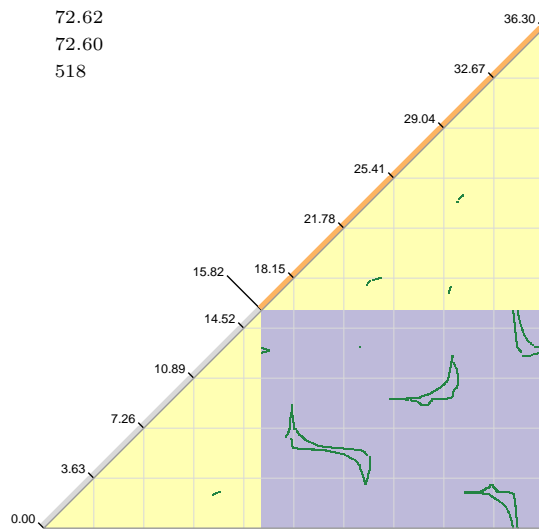
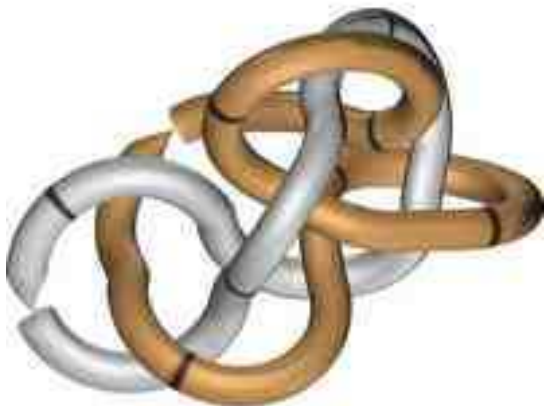
6_1^3



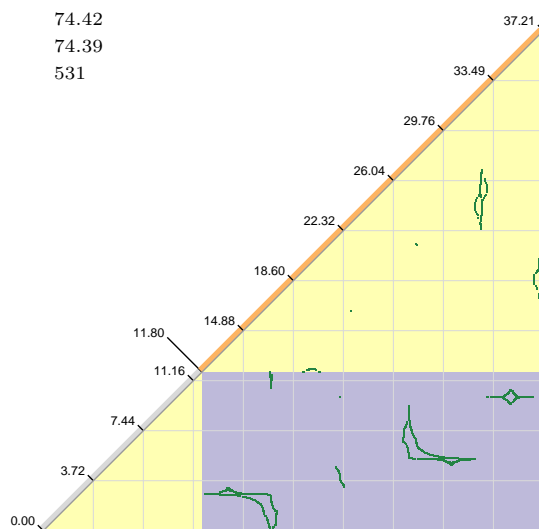
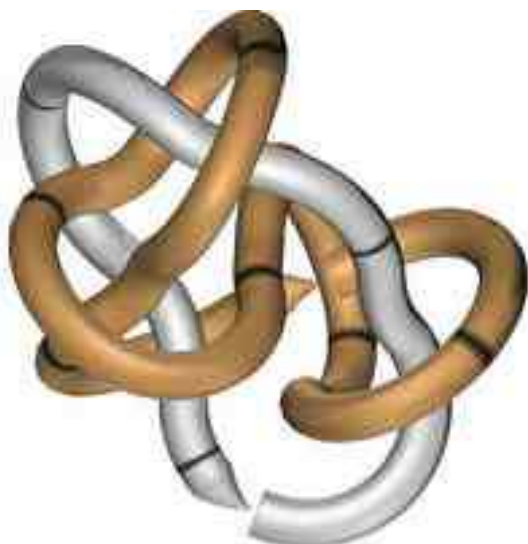
7_4^2



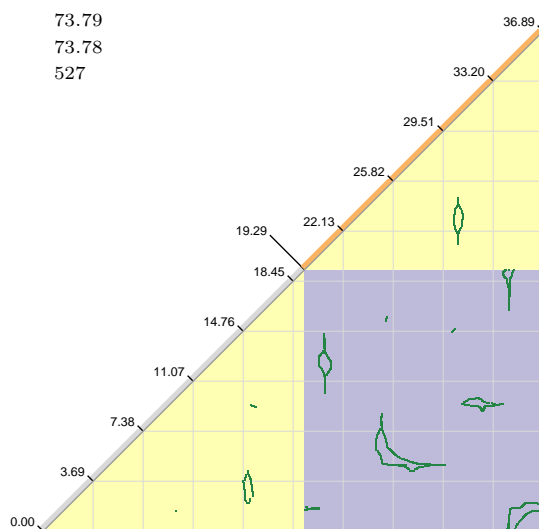
8^2_4



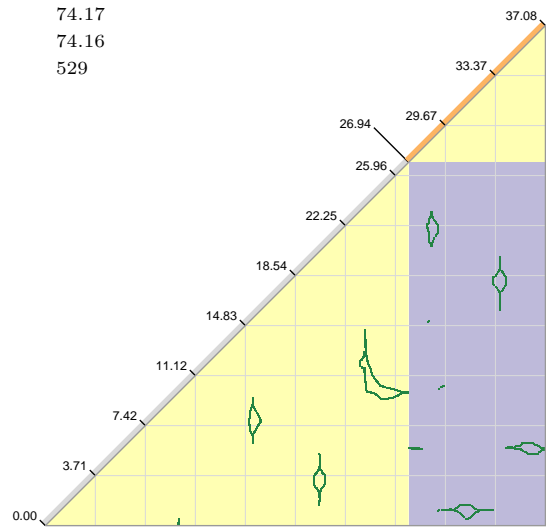
8^2_7



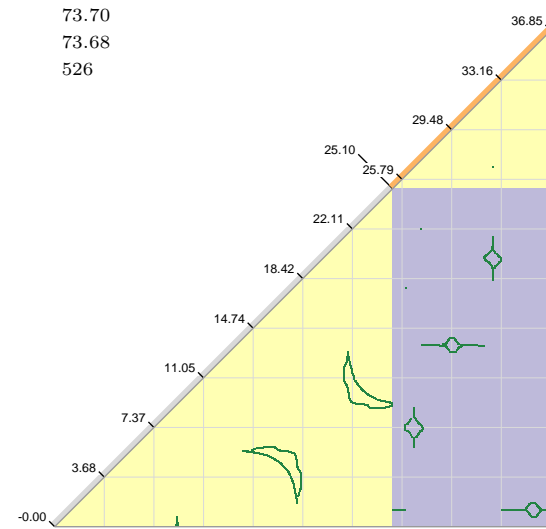
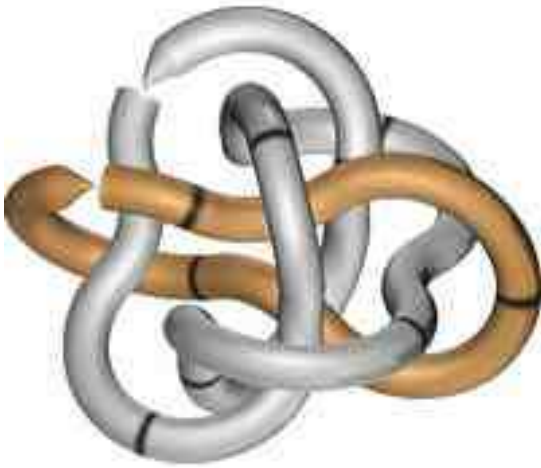
8^2_8



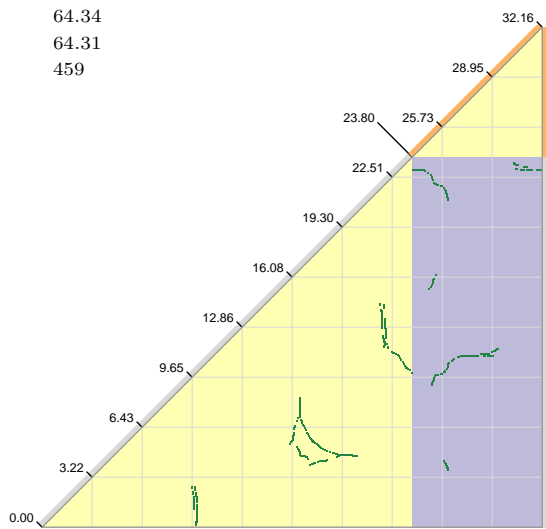
8^2_{13}



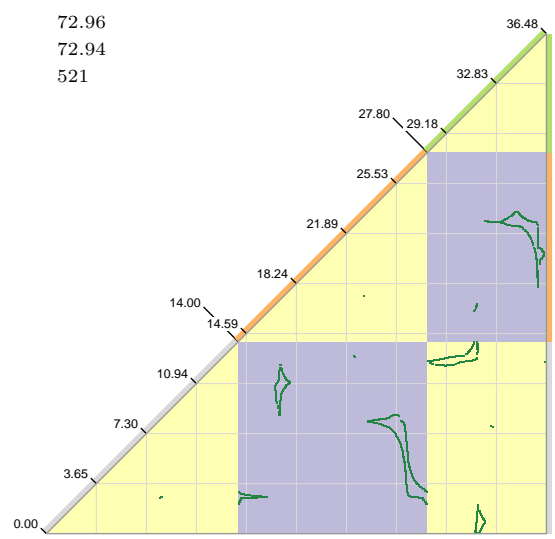
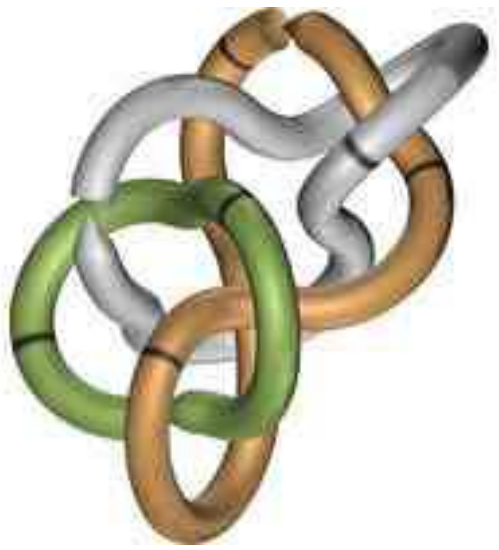
8^2_{14}



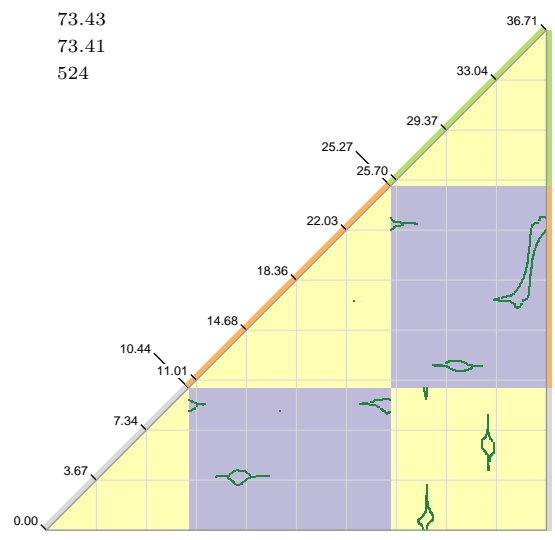
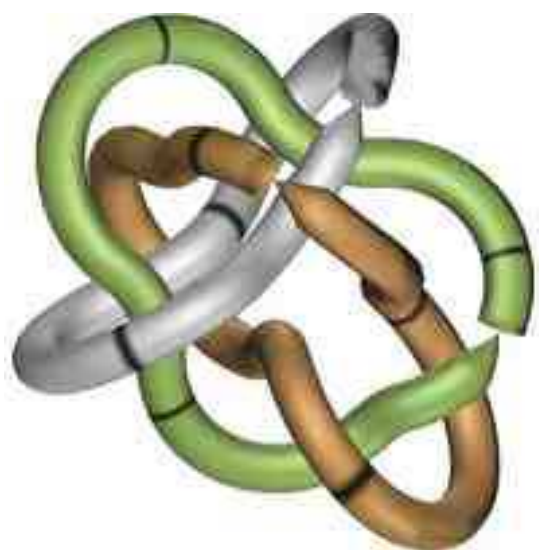
8^2_{15}



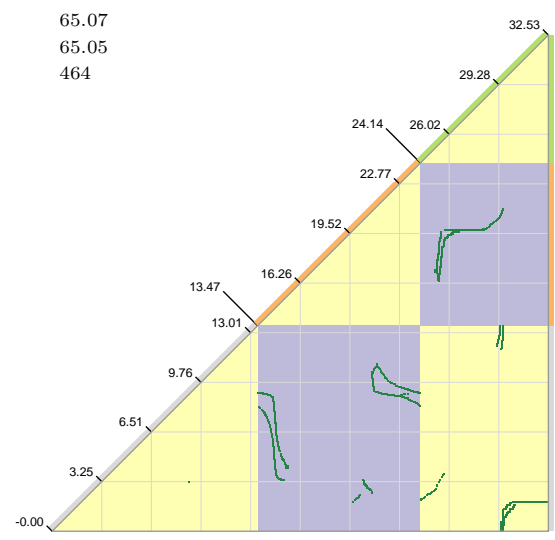
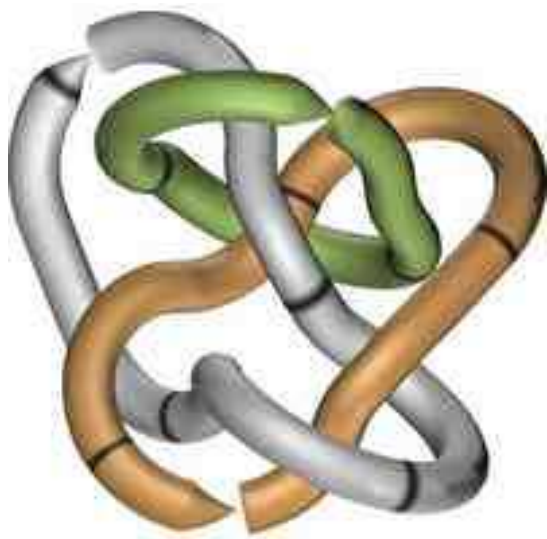
∞_2^3



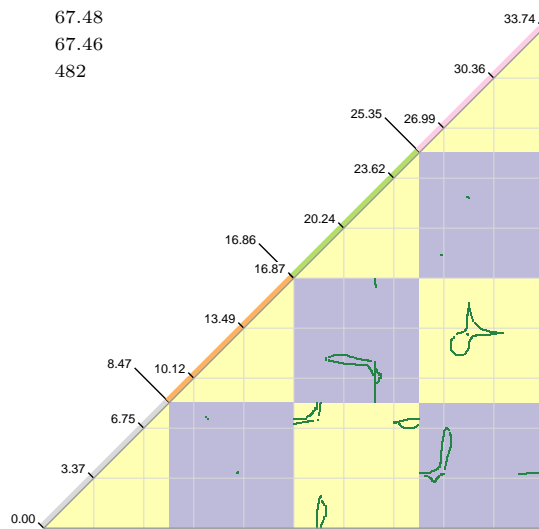
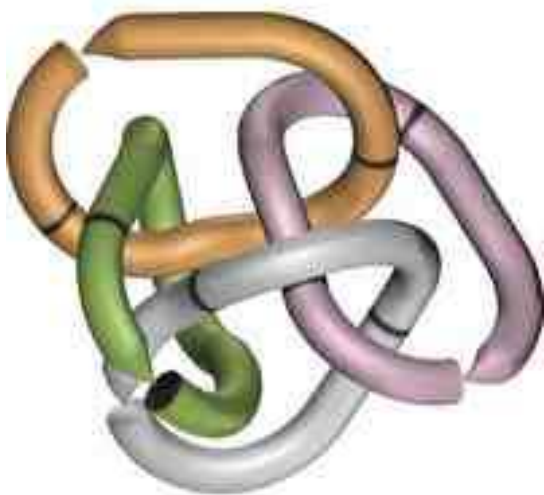
∞_5^3



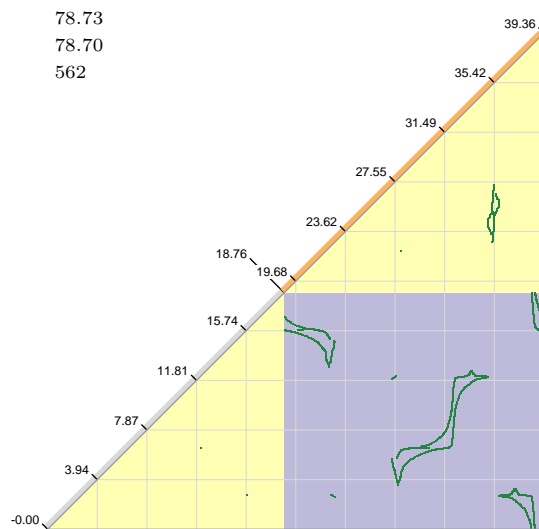
∞_8^3



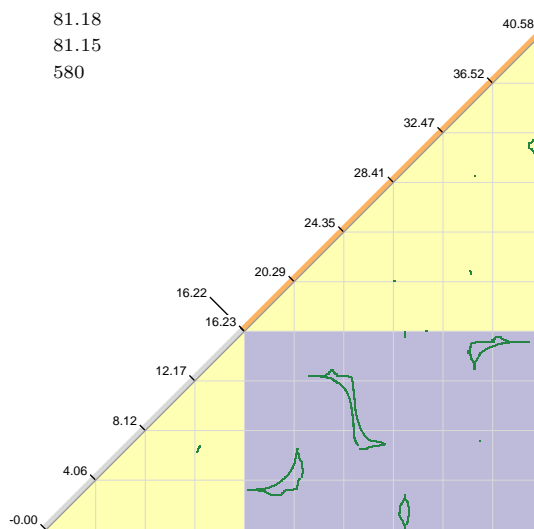
8^4_2



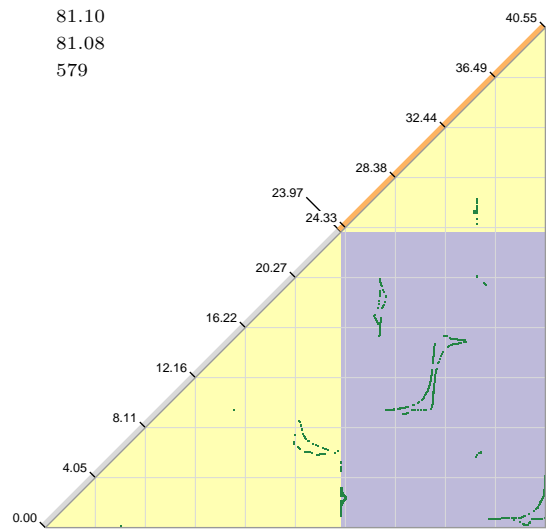
9^2_4



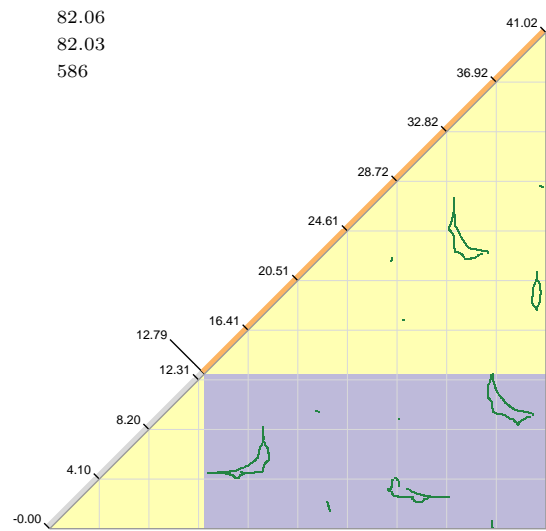
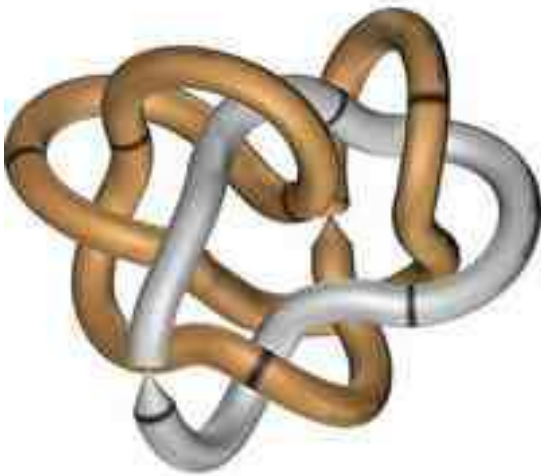
9^2_7



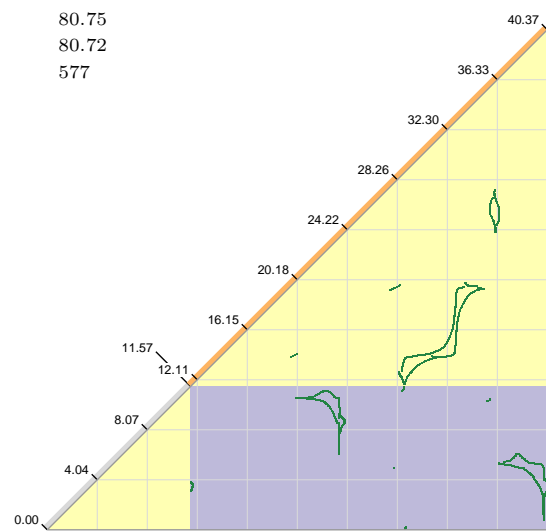
9^2_8



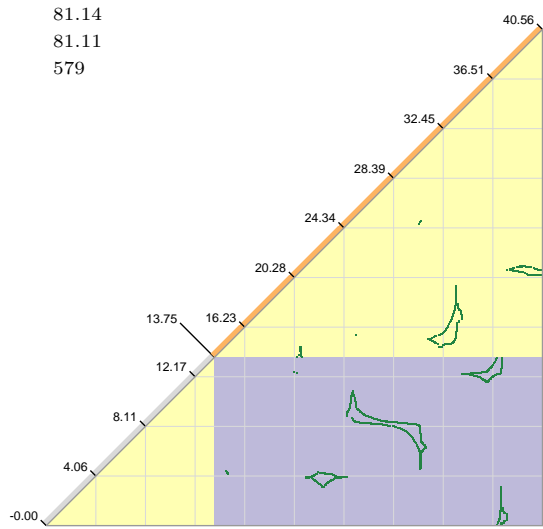
9^2_{11}



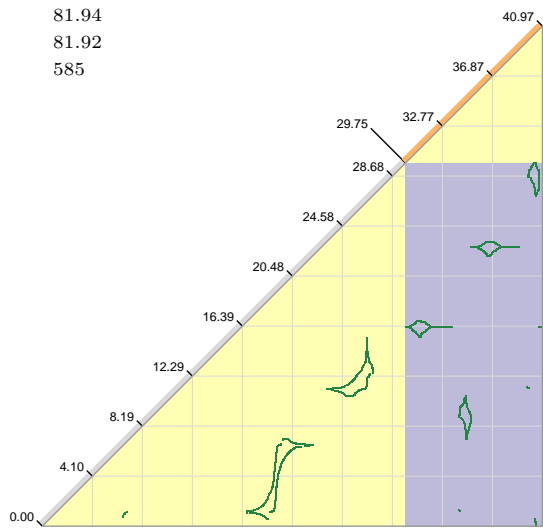
9^2_{14}



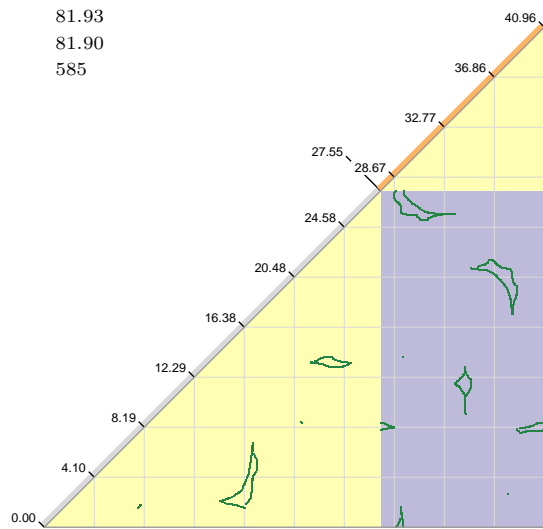
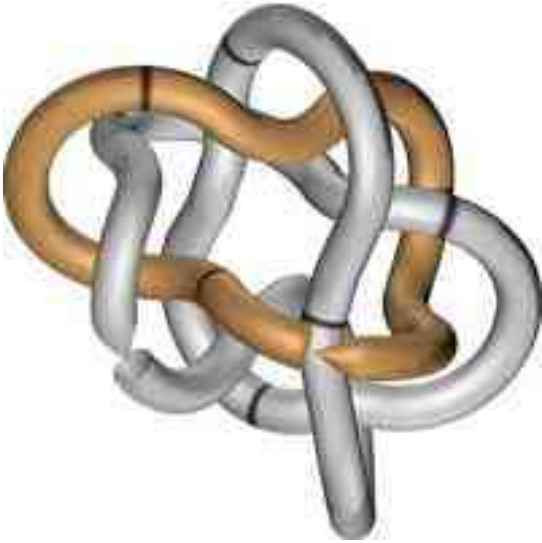
9^2_{22}



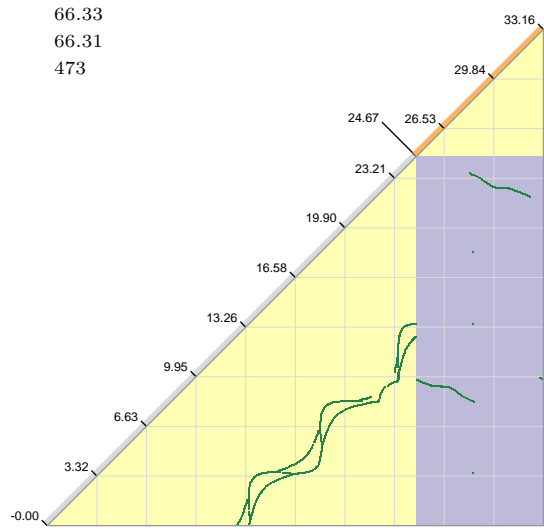
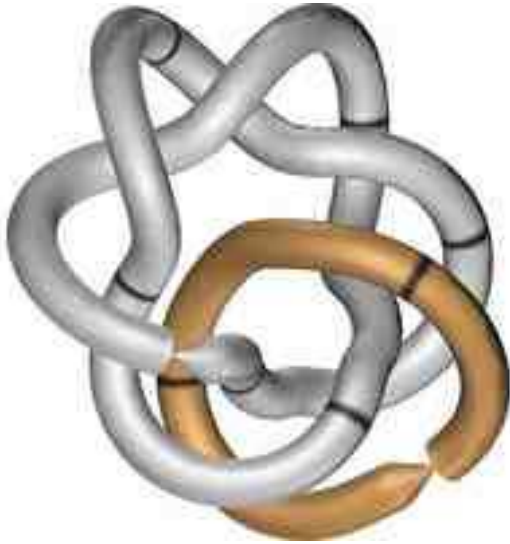
9^2_{37}



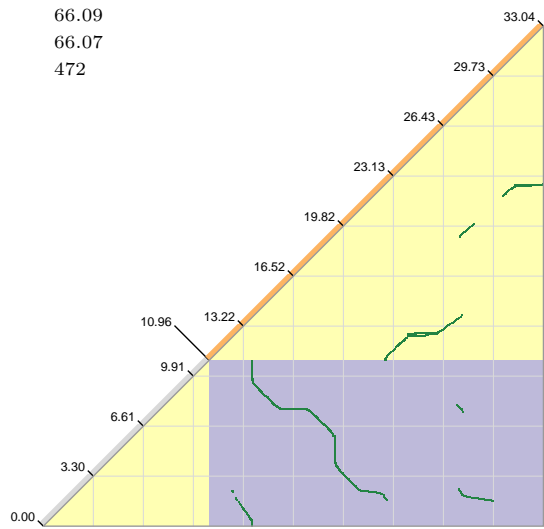
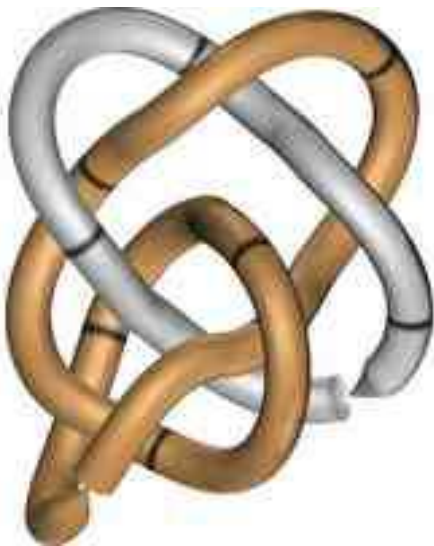
9^2_{39}



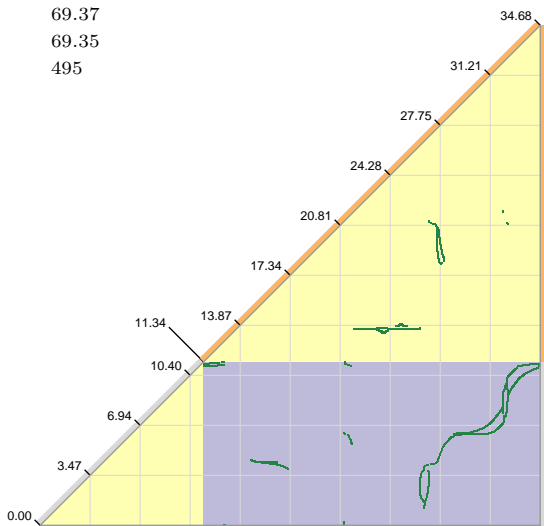
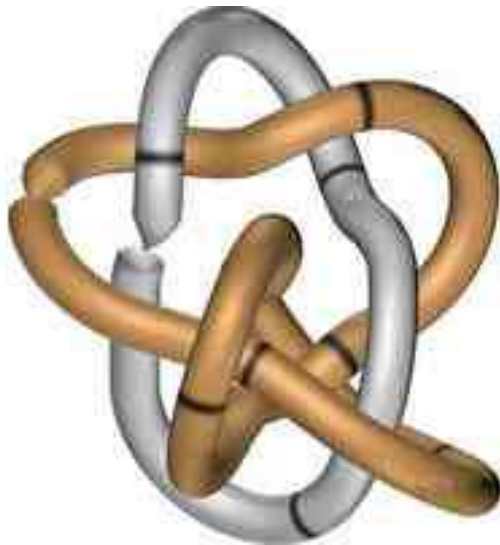
9^2_{43}



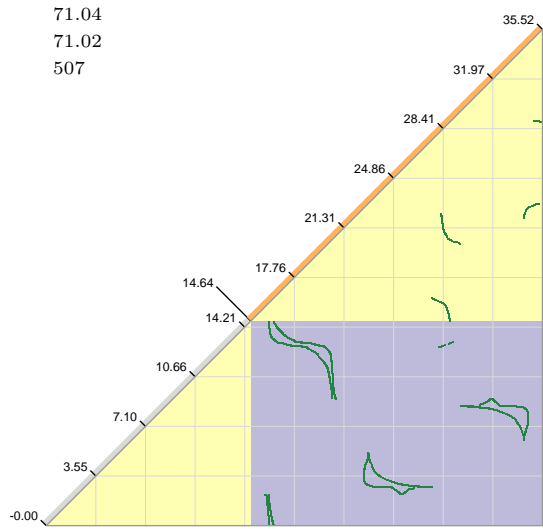
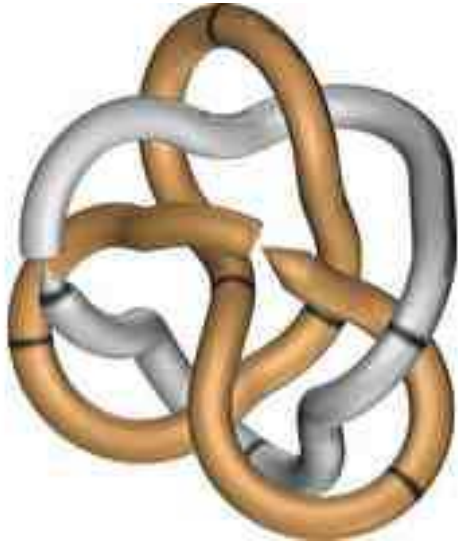
9^2_{49}



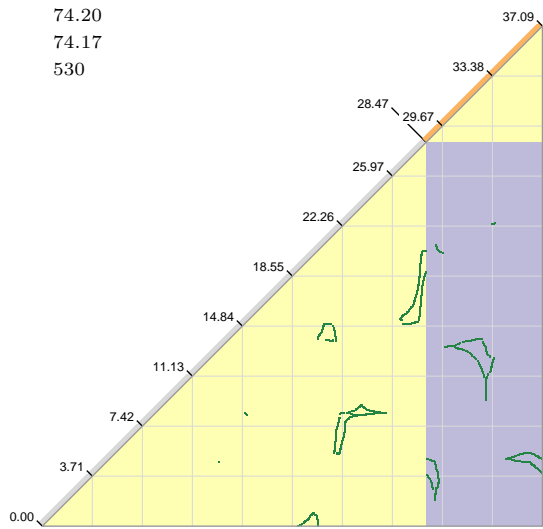
9^2_{50}



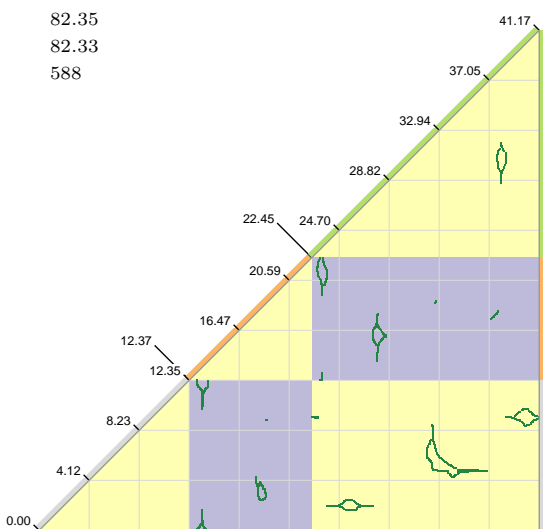
9^2_{54}



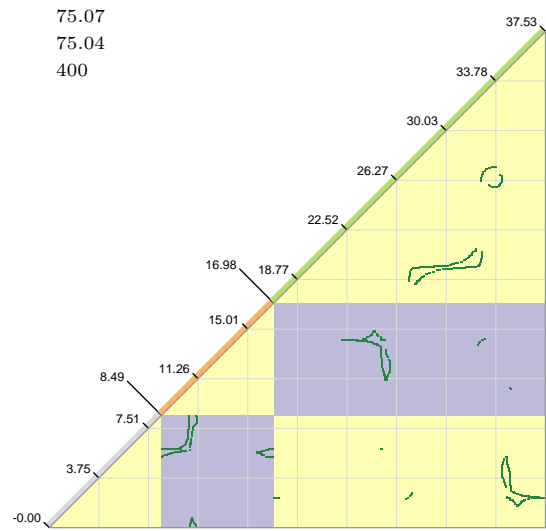
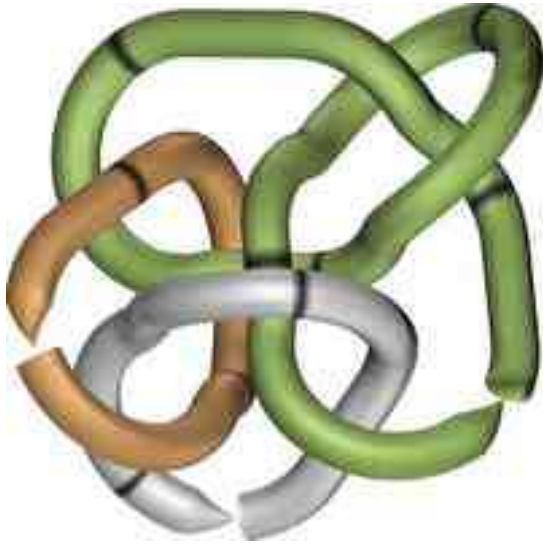
9^2_{58}



9^3_{10}



9^3_{16}



9^3_{21}

